AIAA 81-1254R

A Subsonic Panel Method for Iterative Design of Complex Aircraft Configurations

J. B. Malone*
Lockheed-Georgia Company, Marietta, Georgia

An iterative-design method for the generation of wing geometries with specified surface-pressure distributions is described. The design method is an adaptation of the well-known surface-transpiration technique for approximating boundary-layer effects. A velocity distribution normal to the aircraft surface is sought which minimizes the difference between computed and desired pressures. The transpiration distribution for a given initial wing geometry is determined by numerical optimization and is then used to reloft the configuration. The use of this iterative procedure with a subsonic surface-singularity panel method is illustrated for several example design problems.

I. Introduction

DURING the past decade, several panel methods[1-6] have been developed which can be used to determine the potential flowfield about realistic aircraft shapes. These computational methods provide the needed capability for accurately modeling the aerodynamic interference effects of arbitrary geometries such as multiple lifting surface and/or wing-body configurations. Viscous effects for weak interaction flow conditions can also be approximated by the incorporation of suitable boundary-layer computational methods.[1]

Although originally developed for direct aerodynamic analysis applications, panel methods can also be used to solve the inverse or design problem. In the latter case, an aircraft geometry must be determined which satisfies certain specified design criteria. Examples of often used criteria are the achievement of minimum induced drag[5] or the generation of a desirable surface-pressure distribution.[7]

Design methods based entirely upon the use of lifting surface panel codes are easily developed and computationally efficient.[5,8,9] However, for problems such as the design of wing-body fillets or thick wing sections, lifting surface methods alone cannot be expected to provide the required computational capability. Therefore current research efforts have focused on the development of design procedures which utilize surface-singularity panel methods. These newer design techniques are, in general, iterative procedures due to the nonlinear nature of the inverse problem solved using nonplanar panel codes.

Recently published design procedures differ significantly in both the method of problem solution and the degree of approximation assumed. For example, the method described in Ref. 10 is a noniterative, single-step utilization of existing planar and nonplanar panel codes. In this technique, aerodynamic interference effects are first determined with the surface-singularity analysis code, and then used to modify target pressures input to a planar inverse procedure. Beatty and Narramore[11] have developed a two-dimensional airfoil design method which has been extended to three-dimensional flow cases.[12] This procedure also combines planar and nonplanar panel codes, but permits a design match only for upper (or lower) surface pressures. The iterative-design method provided with the PANAIR code,[13] while accurately accounting for interference effects, requires the starting geometry to be close to the desired design configuration. This requirement arises from the linear approximation used to obtain a target tangential-flow vector during each design cycle. Bristow[14] has developed a two-dimensional method in which an accurate velocity-geometry perturbation relationship is used to redesign a basic starting configuration. This method is currently being extended to three-dimensional flows, but at this writing is not available to industry. Finally, Fray and Slooff[15] have developed a design method, which, although incorporating lifting surface theory, is capable of thick wing design.

Presented as Paper 81-1254 at the AIAA 14th Fluid and Plasma Dynamics Conference, Palo Alto, Calif., June 23-25, 1981; submitted July 15, 1981; revision received Nov. 30, 1981.

*Scientist. Member AIAA.

II. Design Procedure Objectives

The iterative-design procedure which is the subject of this paper was developed to satisfy several different design objectives. First, a design procedure was required which could generate realistic final geometries representing arbitrary camber, twist, or thickness variations relative to a basic starting configuration. This capability is desirable since it relaxes the need to know, a priori, a starting geometry which would be close to the final converged design shape. Second, a method was sought which was suitable for the design of local regions of aircraft geometry such as wing-body fillets or fuselage gear-pod surfaces. The satisfaction of this objective required a design method which was not limited to wing design alone, but could be extended to permit the design of nonlifting body surfaces. Third, a method was needed which could easily be applied to next-generation panel methods as new codes become available. This final objective was necessary to insure that the design procedure would reflect current state-of-the-art methods in computational aerodynamics.

At first glance, these design method objectives would seem to be satisfied by the application of numerical optimization techniques which have been used successfully for transonic wing design.[7] Following these (now standard) numerical optimization practices, isolated regions of the aircraft could be designed by choosing a local set of geometric design variables. In addition, the capability for program update would be assured since optimization procedures normally require little interface with the user supplied aerodynamics routines. Unfortunately, a numerical optimization scheme requiring the use of geometry-perturbation design variables, such as the polynomial functions utilized by Lores,[7] would be prohibitively expensive when coupled with a surface-singularity panel method. However, the use of an op-

timization directed design procedure can be made feasible by choosing a different type of design variable which does not require the recalculation of aerodynamic influence coefficient matrices (AICS) during a given cycle of the iterative-design process.

III. Optimal-Surface-Transpiration Design Method

An iterative-design procedure has been developed which utilizes numerical optimization techniques to generate wing-body geometries with prescribed surface-pressure distributions. The design method is an adaptation of the well-known surface-transpiration technique[16] for approximating boundary-layer effects. Specifically, a surface flow-through velocity distribution normal to the body surface is sought which minimizes the difference between computed and desired pressures.

The optimum-transpiration distribution for a given starting geometry is determined by a gradient directed search algorithm. The resulting normal-wash distribution is then used to reloft the configuration, thus completing one cycle of the design process. Using relofted geometry from the previous cycle as a new starting configuration, this procedure can be repeated until the specified design criteria have been achieved.

A flow chart for the design method is shown in Fig. 1. Detailed discussions of the major elements of the procedure are given in the following paragraphs.

Mathematical Background

The surface-singularity methods referenced previously are based on linear superposition principles. Aircraft geometries are represented by an assemblage of finite elements, or panels, over which a local singularity distribution is assumed to exist. Each singularity distribution is given as a function of an arbitrary number of unknown parameters. The type of singularity used, as well as its assumed distribution function on each aerodynamic element, depends upon the panel method in question. Source,[1] doublet, and vortex[5] distributions, as well as combinations of these,[2,4] have been used successfully.

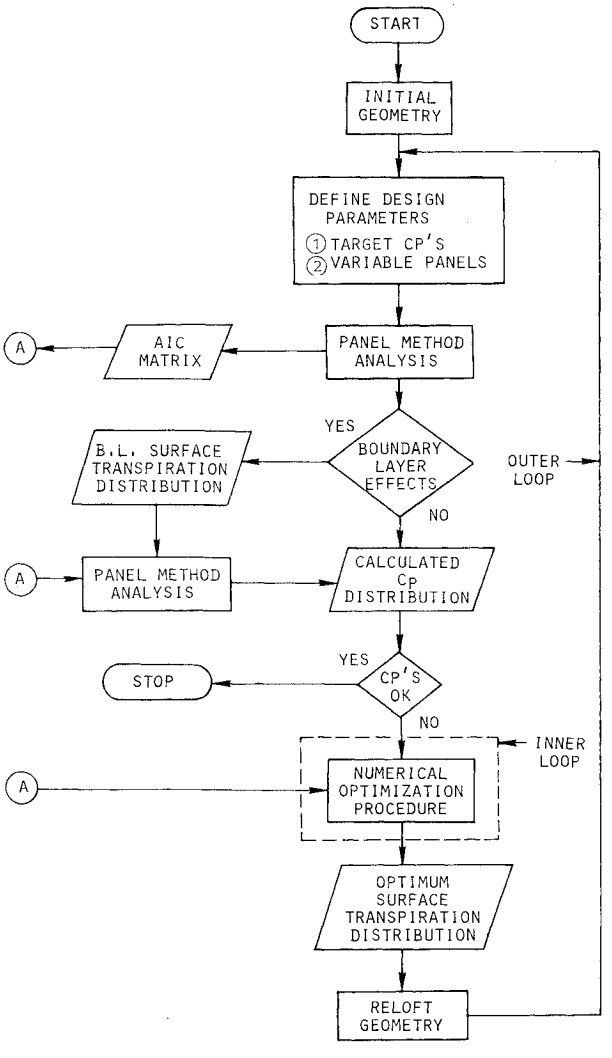

Fig. 1 Flow chart of optimal-surface-transpiration design procedure.

By applying a known boundary condition at control points on the geometry surface for each unknown singularity parameter, a set of linear algebraic equations is obtained. The ith equation of this set can be written as follows:

$$[\boldsymbol{n}_{(i)} \cdot \{\boldsymbol{V}_{ij}\}]\{\xi\} + \boldsymbol{n}(i) \cdot \boldsymbol{U}_\infty = \boldsymbol{n}_{(i)} \cdot \boldsymbol{W}(i) \tag{1}$$

where $\{\boldsymbol{V}_{ij}\}$ are the velocity vectors induced at the ith control point by the jth singularity parameter; $\boldsymbol{U}_\infty$ is the freestream velocity vector; $\boldsymbol{n}(i)$ is the unit normal vector at the ith control point; $\boldsymbol{W}(i)$ is the total velocity vector at the ith control point; and $\{\xi\}$ are the unknown singularity parameters.

The solution to the full set of equations can be obtained by conventional matrix inversion methods. Thus

$$\{\xi\} = [\mathrm{AIC}] \cdot (-[\boldsymbol{n}] \cdot \{\boldsymbol{U}_\infty\} + \{\boldsymbol{W}_N\}) \tag{2}$$

where [AIC] is the aerodynamic influence coefficient matrix, and $\{\boldsymbol{W}_N\}$ is the total velocity magnitude normal to body surface at panel control points (positive in direction of outward facing normal).

Once the singularity parameters, ξ, are known, flowfield properties such as local velocity and surface-pressure coefficients, C_p, are easily determined by the following relationships:

$$\{\boldsymbol{V}_T\} = [\boldsymbol{V}_{ij}] \cdot \{\xi\} \tag{3}$$

$$C_{p_i} = 1.0 - |\boldsymbol{V}_{T_{(i)}}|^2 \tag{4}$$

Inviscid flow solutions are obtained from Eq. (2) by first setting $\{\boldsymbol{W}_N\}$ to zero, thereby enforcing a flow-tangency boundary condition at the panel control points. Viscous effects can also be approximated by solving a second potential flow problem with an appropriate normal velocity distribution, $\{\boldsymbol{W}_N^{BL}\}$, included in Eq. (2). This method of viscous simulation is known as the surface-transpiration technique or the method of equivalent sources. Questions of computational accuracy aside, this approach to viscous simulation is appealing since the original AIC matrix in Eq. (2) is reused in subsequent calculations.

Design Variable Selection

The design variables used in the present iterative procedure are perturbations of the total normal velocity vector $\{\boldsymbol{W}_N\}$. This incremental velocity distribution, denoted by $\{\delta\boldsymbol{W}_N\}$, can be introduced into Eq. (2). Then,

$$\{\xi_p\} = [\mathrm{AIC}] \cdot (-[\boldsymbol{n}] \cdot \{\boldsymbol{U}_\infty\} + \{\boldsymbol{W}_N^{BL}\} + \{\delta\boldsymbol{W}_N\}) \tag{5}$$

and

$$\{\xi_p\} = \{\xi\} + \{\delta\xi\} \tag{6}$$

where $\{\xi_p\}$ is the total singularity distribution, and $\{\delta\xi\}$ is the incremental singularity distribution due to a perturbation $\{\delta\boldsymbol{W}_N\}$. It can be seen from Eqs. (5) and (6) that

$$\{\delta\xi\} = [\mathrm{AIC}]\{\delta\boldsymbol{W}_N\} \tag{7}$$

Surface-pressure coefficients are likewise obtained by substituting $\{\xi_p\}$ for $\{\xi\}$ in Eq. (3). Thus changes in pressure due

to perturbations in design variables can be determined using a single aerodynamic-influence-coefficient matrix.

The choice of which elements of $\{\delta W_N\}$ are to be used as design variables is completely arbitrary. Isolated areas of surface geometry can be designed by setting to zero the elements of $\{\delta W_N\}$ which act on panels outside the region of interest. Thus an examination of Eq. (7) shows that only columns of the [AIC] matrix corresponding to active design-variable panels are required for the calculation of $\{\delta\xi\}$.

Objective Function Definition

The *value* or *objective* function for the present design procedure is defined as

$$E=\left[\left(\sum_{i=1}^{N} W(i)\,[C_{p_t}(i)-C_{p_c}(i)]^2\right)\Big/N\right]^{1/2} \tag{8}$$

where $C_{p_t}(i)$ is the target pressure on the ith panel; $C_{p_c}(i)$ is the calculated pressure on the ith panel; $W(i)$ is the weight function on ith panel; and N is the total number of target panels. For each evaluation of the objective function, the calculated pressure coefficients are obtained using Eqs. (5), (3), and (4).

The weight function is constant for each target-pressure panel. Bristow[14] uses arclength weight factors in his two-dimensional design method. A corresponding weight function for the present three-dimensional method would be the individual panel areas. Optionally, the design engineer may specify arbitrary panel-weight factors which reflect the relative importance of each target pressure.

It should be noted here that target-pressure panels are not required to correspond to design-variable panels in either location or total number. Thus the effects of design-variable changes on the pressures of nearby, fixed surface regions can be included in the design process.

Numerical Search Procedure

As shown in Fig. 1, each cycle of the present iterative-design procedure contains an inner iteration loop. The purpose of this inner loop is to determine an incremental surface-transpiration vector, $\{\delta W_N\}$, which will minimize the error function defined by Eq. (8). This optimal-surface-transpiration distribution is obtained by the application of numerical optimization methods as described below.

The numerical optimization algorithm used in this study is a gradient directed search procedure. Each iteration of the optimization loop requires the calculation of derivatives of the objective function with respect to changes in design variables. As discussed previously, the normal velocities at specified panel centroids are used as independent design variables. Finite-difference derivatives for the kth optimization iteration are calculated by perturbing the ith component of $\{W_N\}^k$, denoted by $\Delta W_N^k(i)$, while setting all other $\Delta W_N^k(j)$, $j\neq i$ to zero. A gradient vector, $\{g\}^k$, is then constructed by sequentially perturbing all of the active design variables. Thus the ith component of the gradient vector can be written as follows:

$$g^k(i)=\Delta E^k(i)\,/\,|\Delta W_N^k(i)| \tag{9}$$

where

$$\Delta E^k(i)=E(\{W_N\}^k+\{\Delta W_N\}^k)-E(\{W_N\}^k) \tag{10}$$

and $|\Delta W_N^k(i)|$ is the magnitude of the ith design variable perturbation.

In Eq. (10) the vector $\{W_N\}^k$ represents the algebraic sum of the boundary-layer transpiration distribution $\{W_N^{BL}\}$ and the incremental distribution $\{\delta W_N\}^{k-1}$ determined by the previous optimization iteration. That is,

$$\{W_N\}^k=\{W_N^{BL}\}+\{\delta W_N\}^{k-1} \tag{11}$$

The distribution $\{W_N^{BL}\}$ is calculated for the starting geometry of each iterative-design cycle (i.e., outer iteration loop) and is held fixed during the inner optimization loop.

The gradient vector of the kth optimization iteration is used to determine a feasible direction in design-variable space which will decrease the value of the objective function. That is,

$$\{\delta W_N\}^k=\{\delta W_N\}^{k-1}+\alpha\{d\}^k \tag{12}$$

where $\{d\}^k$ is the search direction vector, or

$$\{d\}^k=f(\{g\}^k) \tag{13}$$

and α is the step size along the direction vector.

The functional relationship defined by Eq. (13) depends upon the specific optimization method employed for the numerical search. For the present study, the well-known steepest descent method[17] was used to determine optimum-surface-transpiration distributions.

In the steepest descent method the search direction lies along the gradient vector and is given by

$$\{d\}^k=-\{g\}^k \tag{14}$$

For each search direction, $\{d\}^k$, a value of α must be determined which minimizes the objective function, E. During this phase of the optimization process, a line search is performed by holding $\{d\}^k$ constant and gradually increasing from zero the value of α used in Eq. (12) until an *overshoot*, or increase, in E occurs. Then a quadratic predictor is used to estimate a new value of α. Normally, two or three quadratic predictor steps will provide a good estimate for the optimum α parameter. Once α has been fixed, a new gradient vector can be determined for the next optimization iteration.

The number of optimization iterations required for convergence within a given iterative-design cycle is somewhat arbitrary. Most numerical search algorithms require at least one iteration for every active design variable. However, in practice, considerably fewer iterations are needed to produce a good approximation to the optimum-surface-transpiration distribution.

Calculation of New Surface Geometry

A new aircraft surface geometry is calculated as the final step of each iterative-design cycle. Once an optimal-surface-transpiration velocity distribution has been determined, the new geometry is obtained by applying the conservation of mass principle to the flowfield about the starting geometry. As discussed by Tranen[18] for two-dimensional flow, a pseudo displacement thickness can be calculated by integrating Lighthill's expression for equivalent sources. Then,

$$\delta^*=\frac{1}{\rho V_t}\left\{\int_0^s \rho W_N\,ds+\text{const}\right\} \tag{15}$$

where δ^* is the displacement thickness; W_N is the normal velocity at surface; V_t is the tangential velocity at surface; ρ is the fluid density; and s is the surface arclength.

For the present relofting procedure, a pseudo boundary layer is calculated in a two-dimensional strip manner using Eq. (15). Values of displacement thickness are calculated at panel centroids and then used to translate the original panel geometry in space along its unit normal direction. Thus

$$R'(x,y,z)=R(x,y,z)+\delta^*\cdot\boldsymbol{n} \tag{16}$$

where $R'(x,y,z)$ is the new position vector of panel cornerpoint; $R(x,y,z)$ is the original position vector of panel cornerpoint; and $\boldsymbol{n}$ and δ^* are defined as in Eqs. (1) and (15).

Owing to variations in δ^*, adjacent panel cornerpoints which were originally coincident, translate to different points

in space after application of Eq. (16). To eliminate this problem, simple averaging is used to recover coincident points.

A second, frequently occurring problem in design applications is the generation of undesirable open, or fishtail, trailing-edge geometries. This problem is effectively, if not somewhat artificially, alleviated by the removal or addition of airfoil thickness along the chord to enforce a specified trailing-edge thickness constraint. Modifications to the surface ordinates are wedge shaped, starting from zero at the airfoil leading edge and increasing to a maximum at the trailing-edge location.

IV. Implementation of the Design Method

An existing subsonic panel code, developed by Hess,[19] has been modified to incorporate the iterative-design procedure described in the previous section. The most recent version of the code, made available through COSMIC, solves the incompressible potential-flow problem for arbitrarily configured flight vehicles. In addition to other features, the COSMIC version of this code includes the equivalent source technique as one method for simulating viscous effects. As a result, only a minimum of additional coding effort was required to develop a pilot design procedure option for the panel method.

V. Sample Results and Discussion

Two example design problems are discussed to illustrate the use of the present iterative-design procedure. The cases presented are for incompressible, inviscid flow conditions. The airfoil ordinate scales for geometry plots are magnified to aid in visualizing contour differences.

The first problem considered is that of a single lifting strip at angle of attack to the freestream velocity. The strip geometry corresponds to a symmetric NACA 0015 airfoil section and is modeled with 30 aerodynamic panels, evenly divided between upper and lower surfaces. The span of the lifting strip is 10% of the chord dimension and a reflection plane has been defined at the inboard edge of the strip. The normal velocity at each panel centroid is taken as an independent design variable and target pressures, likewise, are applied at all aerodynamic panels.

The ability of the design procedure to reproduce a known geometry corresponding to a specified pressure distribution is illustrated in Figs. 2-7. Target pressures were calculated for a similar lifting strip with a NACA 2412 airfoil section and applied to the thicker, symmetric strip. A total of six iterative-design cycles was required to achieve reasonable target pressure convergence. During each design cycle, only five normal velocity optimization iterations were requested. The initial and target pressure distributions for this case, as well as the corresponding airfoil geometries, are shown in Figs. 2 and 3.

Figures 4 and 5 illustrate the actual airfoil pressures and geometry determined at the end of the first design cycle. At this point in the design process, a cambered airfoil shape has been generated, but the effective angle of attack is in error. Surface pressures and a comparison of airfoil geometries at the end of the final design cycle are presented in Figs. 6 and 7.

No surface-contour smoothing was performed during the design process. However, an examination of Fig. 7 shows that the trailing-edge region on the lower surface of the final geometry would be improved by appropriate contour modifications. Owing to the iterative nature of the design process, necessary smoothing operations can easily be performed prior to the start of any design cycle.

The computed results for a wing-body design problem are presented in Figs. 8-13. The starting configuration consists of a swept wing mounted at midheight on a body of revolution. The wing has a gross aspect ratio of 6 (i.e., wing extended to fuselage centerline), a quarter-chord sweep angle equal to 30 deg, and a taper ratio of one-third.

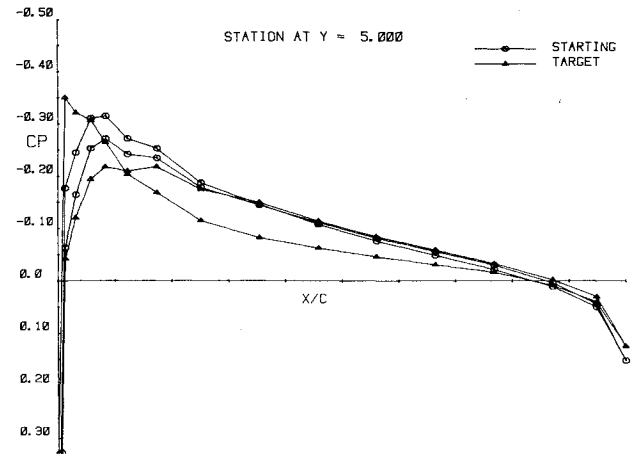

Fig. 2 Comparison of initial pressures (NACA 0015) and target pressures (NACA 2412) for single lifting strip.

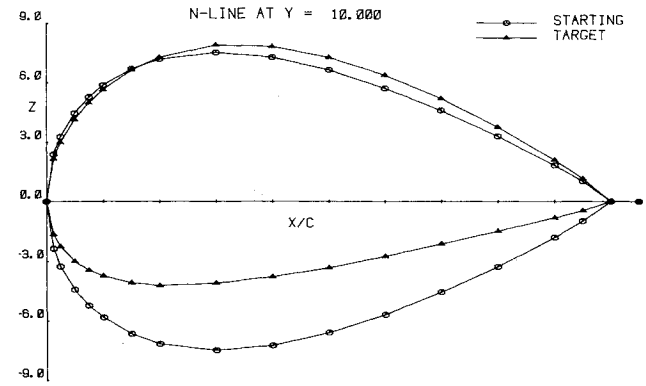

Fig. 3 Comparison of initial geometry (NACA 30015) and target geometry (NACA 2412) for single lifting strip.

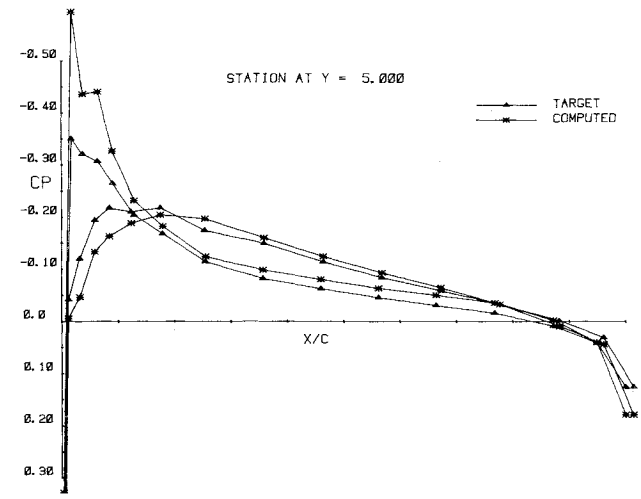

Fig. 4 Pressure distribution on lifting strip after first design cycle.

The aerodynamic paneling arrangement for this wing-body combination is shown in Figs. 8 and 9. A total of 268 surface panels are used to model the aircraft geometry; 160 panels on the wing and 108 panels on the fuselage. The wing-fillet region is modeled as a lifting strip and has highly swept leading and trailing edges.

The target pressure distribution used in this example wing-body design problem was obtained by first computing surface pressures on a similar aircraft configuration for which the wing-root thickness had been increased by 50%. An angle of attack of 3.5 deg was assumed for these calculations. Upper and lower surface pressures on three of the wing lifting strips

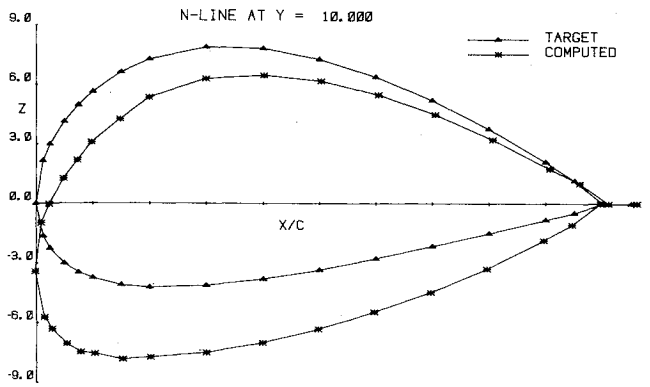

Fig. 5 Airfoil geometry of lifting strip after first design cycle.

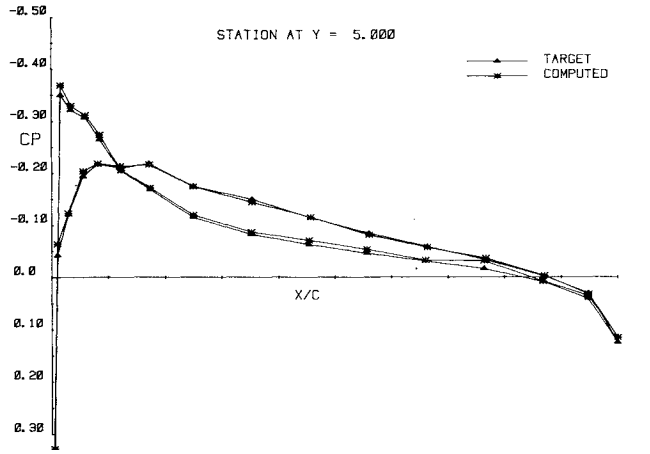

Fig. 6 Surface-pressure distribution on lifting strip after sixth design cycle.

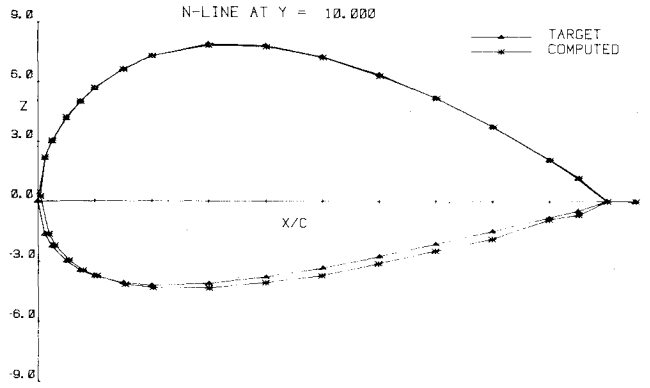

Fig. 7 Airfoil geometry of lifting strip after sixth design cycle.

nearest the fuselage were then utilized as target pressures for the starting configuration shown in Figs. 8 and 9.

Design variables were assigned to aerodynamic panels for the wing lifting strip located in the center of the target-pressure region. During the design process, changes to the shape of sections containing design variables also produce modifications to adjacent strips in the spanwise direction. Thus, for the purposes of this sample problem, modifications to a large surface region (60 panels) were obtained with the use of a minimum number of active design variables (20 variables).

Computed results for the wing-body case are presented in Figs. 10-13. Surface pressures are shown for the wing lifting strip located in the center of the target-pressure area.

Figure 10 shows a comparison of the starting and target-pressure distributions. The increased wing-root thickness of

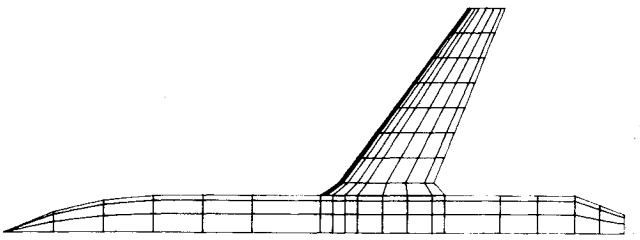

Fig. 8 Aerodynamic paneling for wing-body design problem; planform view.

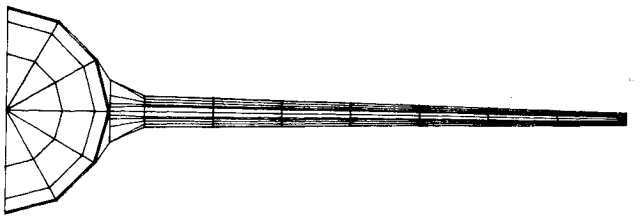

Fig. 9 Aerodynamic paneling for wing-body design problem, front view.

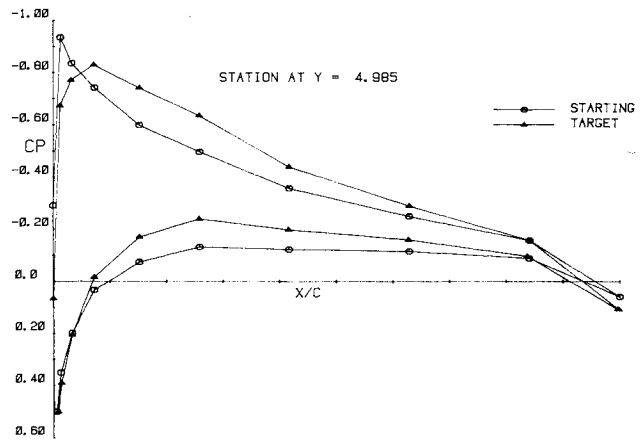

Fig. 10 Comparison of starting and target-pressure distributions for a center lifting strip; wing-body design problem.

the target configuration results in a decrease in the leading-edge suction peak, but an overall increase in suction level everywhere aft of the 10% chord.

The lifting-strip pressures after four iterative-design cycles are presented in Figs. 11 and 12. Figure 11 shows a comparison of pressures computed with the optimal surface-transpiration distribution applied as a boundary condition. Five cycles of numerical optimization were used to determine the final transpiration velocities. As shown in this figure, the calculated pressures compare well with the target distribution forward of the 60% chord. Aft of this location, failure to match the trailing-edge pressure produces a deviation from the target distribution. For this iterative-design cycle, a larger number of optimization iterations would have produced a better pressure correlation in the trailing-edge region.

Figure 12 shows the lifting-strip pressures obtained after reloft of the aircraft geometry has been performed. The target pressure distribution is repeated again for reference purposes. An examination of this figure shows that additional iterative-design cycles would be required to more fully achieve the design criteria. One reason for the slowed convergence rate (compared to previous example) is the approximate nature of the two-dimensional reloft technique used in these computations. A more sophisticated relofting method might improve this step of the present design procedure. In addition, since an optimal-surface-transpiration distribution can be computed for body panels as well as wing panels, an improved

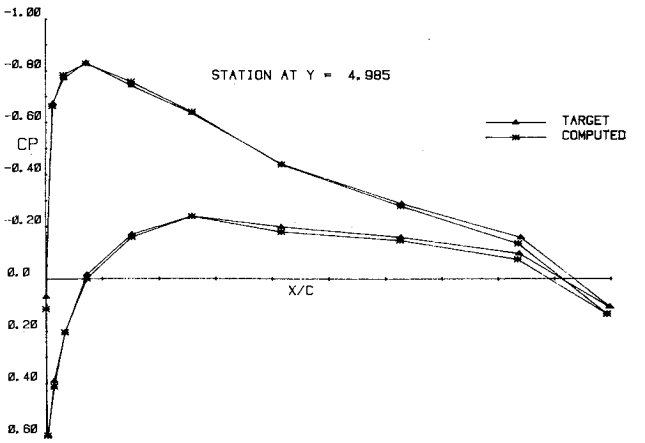

Fig. 11 Lifting-strip pressures including computed surface-transpiration velocities for center lifting strip; fourth cycle of wing-body design problem.

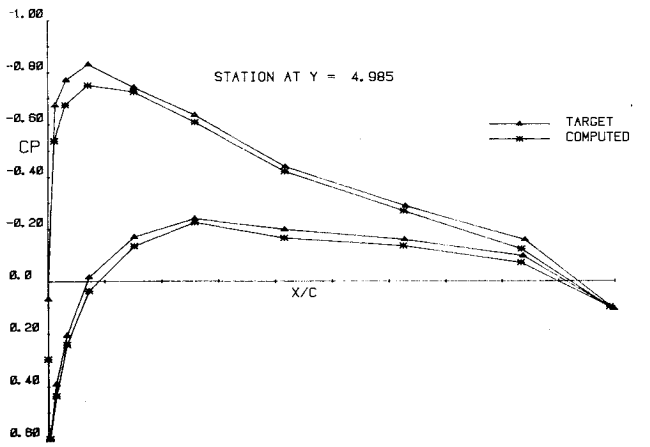

Fig. 12 Lifting-strip pressures after geometry reloft for center lifting strip; fourth cycle of wing-body design problem.

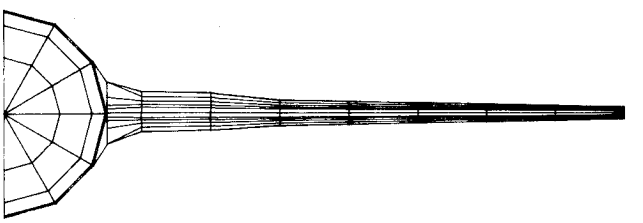

Fig. 13 Wing-body geometry after fourth design cycle; front view.

reloft technique might be devised to permit the design of any portion of the aircraft geometry.

A final result from this wing-body problem is given in Fig. 13. The relofted geometry after the fourth design cycle is shown in a front view similar to that of Fig. 9. The design process has produced a new geometry with a wing-root section approximately 25% thicker than the original starting configuration.

The sample problem results were obtained using a Digital Vax 11/780 minicomputer. A typical design cycle for the wing-body problem required 1 h of CPU time. Approximately 200 objective-function evaluations were computed during each design cycle.

VI. Concluding Remarks

An iterative-design procedure has been developed which is suitable for use with surface-singularity aerodynamic-analysis methods. The procedure has been applied to an existing panel method and results have been presented which illustrate its use in solving design problems. This design procedure should provide a useful tool for the generation of aircraft geometries with specified pressure distributions.

References

[1] Hess, J.L., "A Fully Automatic Potential-Flow Boundary-Layer Procedure for Calculating Viscous Effects on the Lifts and Pressure Distributions of Arbitrary Three-Dimensional Configurations," NSRDC Rept. MDC J7491, June 1977.

[2] Ehlers, F.E., Epton, M.A., Johnson, F.T., Magnus, A.E., and Rubbert, P.E., "An Improved Higher Order Panel Method for Linearized Supersonic Flow," AIAA Paper 78-15, Jan. 1978.

[3] Morino, L., Chen, L.T., and Suciu, E.O., "Steady and Oscillatory Subsonic and Supersonic Aerodynamics Around Complex Configurations," *AIAA Journal,* Vol. 13, 1975, pp. 368-374.

[4] Bristow, D.R. and Grose, G.G., "Modification of the Douglas Neumann Program to Improve the Efficiency of Predicting Component Interference and High Lift Characteristics," NASA CR-3020, Aug. 1978.

[5] Woodward, F.A., Tinoco, E.N., and Larsen, J.W., "Analysis and Design of Supersonic Wing-Body Combinations, Including Flow Properties in the Near Field," NASA CR-73106, Aug. 1967.

[6] Woodward, F.A., "An Improved Method for the Aerodynamic Analysis of Wing-Body-Tail Configurations in Subsonic and Supersonic Flow, Part I—Theory and Application," NASA CR-2228, Part 1, May 1973.

[7] Lores, M.E., Smith, P.R., and Hicks, R.M., "Supercritical Wing Design Using Numerical Optimization and Comparisons with Experiment," AIAA Paper 79-0065, Jan. 1979.

[8] Cenko, A., "Advances in Supersonic Configuration Design Methods," *Journal of Aircraft,* Vol. 17, Feb. 1980, pp. 119-126.

[9] Malone, J.B., "Supersonic Aero Prediction Via Woodward: Analysis and Design Options for the USSAERO Panel Code," Grumman Aerospace Corporation, EG-ARDYN-79-92, Sept. 1979.

[10] Boctor, M.L., Clay, C.W., and Watson, C.F., "An Analysis of Prop-Fan/Airframe Aerodynamic Integration," NASA CR-152186, Oct. 1978.

[11] Beatty, T.D. and Narramore, J.C., "Inverse Method for the Design of Multielement High-Lift Systems," *Journal of Aircraft,* Vol. 13, June 1976, pp. 393-398.

[12] Fornasier, L., "Wing Design Process by Inverse Potential Flow Computer Programs," *The Use of Computers as a Design Tool,* AGARD CP-280, Sept. 1979, pp. 14-1 to 14-14.

[13] Magnus, A.E., Epton, M.A. et al., "PANAIR—A Computer Program for the Prediction of Subsonic or Supersonic Flow About Arbitrary Configurations," Appendix C, Contract NAS2-9830, Jan. 1979.

[14] Bristow, D.R., "A New Surface Singularity Method for Multi-Element Airfoil Analyses and Design," AIAA 80-0330, Jan. 1976.

[15] Fray, J.M.J. and Slooff, J.W., "A Constrained Inverse Method for the Aerodynamic Design of Thick Wings with Given Pressure Distribution in Subsonic Flow," *Subsonic/Transonic Configuration Aerodynamics,* AGARD CP-285, May 1980, pp. 16-1 to 16-9.

[16] Moore, F.K., "Displacement Effect of a Three-Dimensional Boundary Layer," NACA TN 2722, 1952.

[17] Aoki, M., *Introduction to Optimization Techniques,* MacMillan, New York, 1971.

[18] Tranen, T.L., "A Rapid Computer Aided Transonic Airfoil Design Method," AIAA Paper 74-501, June 1974.

[19] Hess, J.L., "Calculation of Potential Flow About Arbitrary Three-Dimensional Lifting Bodies," Douglas Aircraft Company, Rept. MDC J5679-01, Oct. 1972.